

Communication-efficient Federated Graph Classification via Generative Diffusion Modeling

Xiuling Wang

xiulingwang@hkbu.edu.hk
Hong Kong Baptist University
Hong Kong, China

Haibo Hu

haibo.hu@polyu.edu.hk
Hong Kong Polytechnic University
Hong Kong, China

Xin Huang

xinhuang@comp.hkbu.edu.hk
Hong Kong Baptist University
Hong Kong, China

Jianliang Xu

xujl@comp.hkbu.edu.hk
Hong Kong Baptist University
Hong Kong, China

Abstract

Graph Neural Networks (GNNs) unlock new ways of learning from graph-structured data, proving highly effective in capturing complex relationships and patterns. Federated GNNs (FGNNs) have emerged as a prominent distributed learning paradigm for training GNNs over decentralized data. However, FGNNs face two significant challenges: high communication overhead from *multiple rounds* of parameter exchanges and *non-IID data characteristics* across clients. To address these issues, we introduce CeFGC, a novel FGNN paradigm that facilitates efficient GNN training over non-IID data by limiting communication between the server and clients to three rounds only. The core idea of CeFGC is to leverage generative diffusion models to minimize direct client-server communication. Each client trains a generative diffusion model that captures its local graph distribution and shares this model with the server, which then redistributes it back to all clients. Using these generative models, clients generate synthetic graphs combined with their local graphs to train local GNN models. Finally, clients upload their model weights to the server for aggregation into a global GNN model. We theoretically analyze the I/O complexity of communication volume to show that CeFGC reduces to *a constant of three communication rounds only*. Extensive experiments on several real graph datasets demonstrate the effectiveness and efficiency of CeFGC against state-of-the-art competitors, reflecting our superior performance on non-IID graphs by aligning local and global model objectives and enriching the training set with diverse graphs.

CCS Concepts

• Computing methodologies → Distributed computing methodologies.

Keywords

Federated Graph Neural Networks; Generative; Diffusion; Non-IID; Communication-efficient



This work is licensed under a Creative Commons Attribution 4.0 International License.
KDD '26, Jeju Island, Republic of Korea
© 2026 Copyright held by the owner/author(s).
ACM ISBN 979-8-4007-2258-5/2026/08
<https://doi.org/10.1145/3770854.3780262>

ACM Reference Format:

Xiuling Wang, Xin Huang, Haibo Hu, and Jianliang Xu. 2026. Communication-efficient Federated Graph Classification via Generative Diffusion Modeling. In *Proceedings of the 32nd ACM SIGKDD Conference on Knowledge Discovery and Data Mining V.1 (KDD '26), August 09–13, 2026, Jeju Island, Republic of Korea*. ACM, New York, NY, USA, 12 pages. <https://doi.org/10.1145/3770854.3780262>

1 Introduction

In recent years, the ubiquity and complexity of graph-structured data have driven the advancement of Graph Neural Networks (GNNs) [78, 93] across a wide range of fields, e.g., recommender systems [15, 16], social network analysis [12, 54], and biology network analysis [35, 91]. Owing to privacy concerns, commercial competition, and regulatory restrictions, Federated Learning (FL) [14, 27, 46] is designed to enable collaborative learning over decentralized data. FL enables distributed model training among multiple clients while safeguarding local data privacy. There have been considerable research efforts in Federated Graph Neural Networks (FGNNs) [14, 27, 46], which can be categorized into two types [46]: *horizontal FGNNs*, where clients' data share the same node features but possess different node samples, and *vertical FGNNs*, where clients' local data exhibit different node features. This paper focuses on horizontal FGNNs, which typically involve a central server and a set of clients, each possessing a set of graphs. Each client independently trains a local GNN on its own data, then sends model parameters/gradients or node/graph embeddings to the server, which aggregates these inputs to produce the global GNN [14, 26, 46]. In this paper, we focus on graph classification [43, 78] as a global GNN's learning task, which aims to classify unlabeled graphs into different categories. Figure 1 illustrates a toy example of graph classification using FGNNs that clients collaboratively train a global GNN to predict whether a given test graph is toxic or non-toxic by server-client exchanges.

Motivations and challenges. While FGNNs show promise in learning over decentralized graph data, they encounter two major challenges. First, the intensive server-client updates during training cause significant communication overhead [37, 45, 52], especially for large models, bandwidth-limited or offline clients [33, 42], as synchronous processing is often costly. Therefore, we focus on reducing communication overhead by enabling asynchronous processing via diffusion models. Second, the data distribution on different clients may diverge significantly on node features and graph

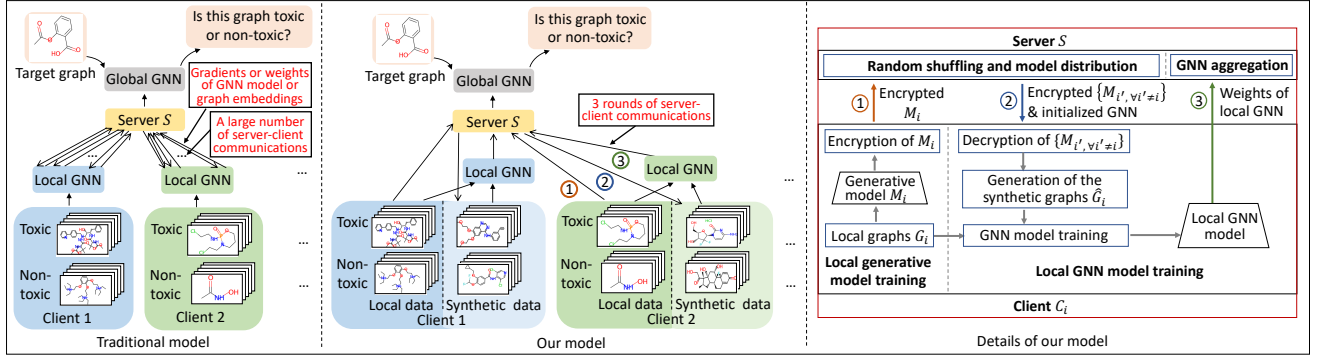


Figure 1: Comparison of the framework of traditional FGNN and our model. The arrows with the numbers ①, ②, and ③ indicate the communication between the server and the clients.

structures [79], which introduces drift in clients' local updates, thereby hindering model convergence and accuracy [17, 76].

To address these challenges, we design CeFGC, a novel framework for graph classification over non-IID graphs that requires only three rounds of server-client communication. Here, we define a server-client communication round as a single exchange of data between the server and clients, in either direction. Briefly, CeFGC is a four-step process. First, each client trains a graph generative diffusion model (GGDM) [5, 84] on its local graphs, which captures the underlying distribution of these graphs. The clients then share these GGDMs with the server (the first round of communication). The server, in turn, redistributes GGDMs and an initialized GNN to clients (the second round of communication). Armed with the received GGDMs, each client generates a set of synthetic graphs and trains a local GNN model using both these synthetic graphs and its local graphs. Subsequently, the clients transmit the weights of their local GNNs to the server (the third round of communication). The server aggregates these weights to obtain the global model. By leveraging GGDMs, CeFGC achieves two key benefits. First, CeFGC not only minimizes the server-client communication rounds but also reduces server-side computation to a single aggregation. Second, it better aligns local objectives with the global model, while also enhancing model's generalization capability by enriching each client's training set with more diverse graphs. These advantages significantly enhance the efficiency and effectiveness of graph classification over non-IID graphs.

Two primary challenges remain for the design of CeFGC. First, since previous GGDMs do not incorporate graph labels into the training process, each client must train one diffusion model per class. This results in high communication bandwidth when transmitting GGDMs in the system, especially with a large number of data classes and clients. The key challenge is how to reduce the number of GGDMs per client while still capturing class-conditional distributions. Second, sharing GGDMs with an honest-but-curious server or other clients poses potential privacy risks, potentially exposing sensitive information of clients' local graphs. Specifically, CeFGC faces two potential privacy risks: (i) the server may attempt to infer the clients' local data from the uploaded GGDMs; (ii) the clients may try to extract sensitive information about other clients' local data from the distributed GGDMs.

To tackle the first challenge, we introduce a label channel into the training process of GGDM, which takes the label of the graph

as input and outputs a noise vector associated with that label. This enables different classes of data to be trained with varying levels of noise within a single diffusion model, allowing each client to train just one model instead of multiple models.

For the second challenge, we have the following solutions. First, each client shares an encrypted GGDM with the server and provides the public key to other clients, ensuring the server cannot infer local data from the uploaded models. Second, the server randomly shuffles the GGDMs before distribution, preventing clients from identifying models' origins. Furthermore, we propose a privacy-enhanced method where the server aggregates each diffusion model with the most similar one before distribution, further mitigating privacy leakage risks. Additionally, it is important to note that common inference attacks [29, 53, 68, 75, 92, 96] or poisoning attacks [4, 50, 56, 85] against FL models are ineffective in our model, as these attacks typically rely on large numbers of communication rounds, such as analyzing gradient or embedding differences between rounds, which is not applicable in our CeFGC.

Our contributions. To the best of our knowledge, this is the first work to design communication-efficient FGNNs for non-IID graph data. In summary, our model introduces two major advancements: first, our model requires only three rounds of server-client communications, efficiently addressing the challenge of communication overhead in traditional FGNNs; and second, by introducing GGDMs to FGNN, each client trains a local GNN based on both the local and synthetic data, and thus effectively improves performance on non-IID graphs across clients. Figure 1 illustrates the key differences between traditional FGNNs and our proposed model. We summarize our main contributions below.

- We introduce CeFGC, a framework that leverages both generative diffusion models and a novel model distribution scheme to minimize the communication overhead of FGNNs while maintaining high model accuracy over non-IID data.
- We modify the existing graph diffusion generative model by incorporating a label channel into the training process, which reduces the communication bandwidth required by the system.
- We conduct comprehensive experiments on three non-IID settings with five real-world datasets from different domains. Our results show that, despite the minimal involvement of only three rounds of server-client communication, CeFGC consistently outperforms the SOTA baselines across different settings.

2 Related Work

FGNNs with non-IID data for graph classification. Recently, several works investigated how to deal with non-IID data with FGNNs. GCFL [79] is a graph-clustered FL framework that clusters clients based on their data heterogeneity, where clients with less data heterogeneity are grouped together. FedStar [72] captures and shares the universal structural knowledge across multiple clients using a particular type of feature-structure decoupled GNN [10], thereby enhancing the local performance of clients in FGNN. GCFGAE [22] integrates FGNN with split learning by dividing the model into portions trained independently by clients and the server. However, GCFGAE focuses on unsupervised learning and is not applicable to our setting. Notably, all the above works face communication overhead, requiring numerous server-client interactions.

Communication efficiency in FL. Numerous works have been introduced to reduce the communication overhead in FL [6, 42, 65, 67], including parameter compression [6, 60, 62], client selection [1, 8, 81], reducing model updates [38, 57, 77], and one-shot FL [21, 95]. However, most of these works focus on learning over non-graph data, leaving the reduction of communication overhead in FGNNs largely unexplored. In summary, the issue of communication overhead in FedGNNs remains unsolved.

Generative diffusion models for graphs. Generative diffusion models have become an emerging generative paradigm for graph generation. The goal of graph generative diffusion models is to learn the underlying distribution of the given graphs and generate novel graphs. The existing studies can be broadly categorized into three classes [11, 89]: (1) *Score-based Generative Models (SGM)* [7, 58] that employ a score function to illustrate the probability distribution of the data; (2) *Denoising Diffusion Probabilistic Models (DDPMs)* [23, 73] that add discrete Gaussian noise to the graph with Markov transition kernels [3] and trains a neural network to predict the added noise to recover the original graph, and (3) *Stochastic Differential Equations (SDEs)* [32, 36, 49] that characterize the development of a system over time under the effect of random noise. We refer the readers to some surveys on generative diffusion models on graphs [11, 89]. This paper uses the pioneer EDP-GNN [58] as the generative diffusion model.

3 Preliminaries

3.1 Graph Neural Network

Consider a graph $G(V, E, X)$ with node set V , edge set E , and node features X , a Graph Neural Network (GNN) aims to learn representations of G by aggregating information from a node's neighbors using neural networks. The learned embedding can be applied to various graph analytics tasks, such as node classification and graph classification. In this paper, we focus on graph classification, which aims to determine the label of an entire graph (e.g., a molecule's toxicity). For this task, all node embeddings will be transformed into a single graph embedding to determine the graph's label.

Most of the existing GNNs follow the message-passing neural network (MPNN) [78] to learn the node embedding. It starts by initializing the node embedding with node features. Each node then receives and aggregates "messages" from its neighbors to form intermediate embeddings. After k steps, each node embedding

incorporates information from its k -hop neighbors. These node embeddings are then aggregated by a *graph pooling operation*, such as max, mean, or hierarchical pooling [24, 86], to form a whole graph embedding [86, 90]. In this paper, we use GIN [82] as the GNN model and mean pooling for aggregation.

3.2 Federated Graph Neural Networks

A Federated Graph Neural Network (FGNN) consists of a server S and a set of N clients $C = \{C_i\}_{i=1}^N$. Each client C_i owns a set of private local graphs \mathcal{G}_i sampled from its own data distribution. S and C will jointly learn a global GNN model over $\mathbb{G} = \bigcup_{i=1}^N \{\mathcal{G}_i\}$. The objective function of the global GNN model is to optimize the overall objectives while keeping private data locally [14]:

$$\min_{\mathbf{W}} \sum_{i=1}^N \mathcal{L}_i(\mathcal{G}_i; \mathbf{W}), \quad (1)$$

where \mathbf{W} represents the parameters of the global GNN, and $\mathcal{L}_i(\mathcal{G}_i; \mathbf{W})$ is the loss (such as cross-entropy loss) over the local graphs \mathcal{G}_i on client C_i . As we consider graph classification as the downstream task, the output of the global GNN is the graph embedding \mathbf{Z}_i for each graph $G_i \in \mathbb{G}$. We assume there are K unique classes within \mathbb{G} , denoted as $Y = \{1, \dots, K\}$. Each graph embedding \mathbf{Z}_i is then used to assign the corresponding graph a label within Y .

3.3 Generative Diffusion Models on Graphs

Graph generation models aim to generate new graph samples that resemble a given dataset. Among these, diffusion-based models have become increasingly popular, which gradually introduce noise into data until it conforms to a prior distribution [7, 23, 32, 36, 49, 58, 73].

Generally, existing graph generative diffusion models (GGDMs) include two processes: (1) the *forward process*, which progressively degrades the original data into Gaussian noise [30], and (2) the *reverse process*, which gradually denoises the noisy data back to its original structure using transition kernels. In this paper, we use Score-based Generative Modeling (SGM) for graph generation. Specifically, given a probability density function $p(x)$, SGM aims to estimate the data score function $\nabla_x \log p_{data}(x)$ in the forward process. It perturbs the data with Gaussian noise of varying intensities and jointly estimates the scores for all noise levels. For each noise level σ , it trains a noise conditional model $s_\theta(x; \sigma)$ to approximate its score function. Then, given a noise distribution $q_\sigma(\hat{x}|x)$, where \hat{x} is a noisy version of x , and a set of noise levels $\{\sigma_l\}_{l=1}^L$, where L is the number of levels, the training loss is defined as:

$$\mathcal{L}(\theta; \{\sigma_l\}_{l=1}^L) = \min_{\theta} \frac{1}{2L} \sum_{l=1}^L \sigma_l^2 \mathbb{E} \left[\left\| s_\theta(\hat{x}_l, \sigma_l) - \nabla_{\hat{x}_l} \log q_{\sigma_l}(\hat{x}_l|x) \right\|_2^2 \right], \quad (2)$$

where \mathbb{E} is the expectation.

In the reverse process, after obtaining the trained conditional score model $s_\theta(x; \sigma)$, synthetic graphs are generated using noise-conditional score networks, such as the Score Matching with Langevin Dynamics model [70]. It is worth noting that although we use SGM-based model in this paper, any other GGDMs that can capture the graph distribution can be adapted to our framework.

4 Details of CeFGC

In this section, we formalize the problem and present our CeFGC.

4.1 Problem Formulation

Given a set of labeled graphs $\mathbb{G} = \bigcup_{i=1}^N \{\mathcal{G}_i\}$, a server S and a set of N clients $C = \{C_i\}_{i=1}^N$. Each client C_i holds a set of private graphs \mathcal{G}_i sampled from \mathbb{G} , with each set following its own data distribution. The objective of our model is to collaboratively train a global GNN, denoted as GNN_{global} , that can perform graph classification, i.e., predicting the label y_{target} of a given graph G_{target} , based on all the \mathcal{G}_i from the clients. This problem can be formalized as follows:

$$GNN_{global} : \{\mathbb{G}, C, GNN_{initial}, G_{target}\} \rightarrow y_{target}, \quad (3)$$

where $GNN_{initial}$ represents the initialization of the GNN model.

Next, we present CeFGC, which incorporates generative models into FGNNS to address the server-client communication overhead and improve the model performance over non-IID graphs. Overall, CeFGC includes four steps: (1) training of the local generative model, (2) transferring of local generative models among server and clients, (3) training of local GNN models, and (4) generation of the global GNN. The rightmost figure in Figure 1 illustrates the steps of CeFGC. Next, we explain the details of each step.

4.2 Phase 1: Local Generative Model Training

We propose two methods for training local generative models: (1) the *basic method*, where each client trains a set of EDP-GNN [58], with each associated to a specific graph class; and (2) the *advanced method*, where each client trains a single generative model over all local graphs using EDP-GNN equipped with a class label channel.

4.2.1 Basic method. For any client C_i , let \mathcal{G}_i be the set of local graphs owned by C_i . First, C_i groups all local graphs in \mathcal{G}_i by their class labels, assigning graphs with the same label to the same group. Let \mathcal{G}_i^k be the set of graphs in \mathcal{G}_i that are associated with the label y_k . Next, C_i trains a set of generative models $\mathcal{M}_i = \{M_{i,k}\}$, each $M_{i,k}$ is trained on all graphs in group \mathcal{G}_i^k . In this paper, we adapt EDP-GNN [58], one of the SGM models for graph generation, to our setting. EDP-GNN trains a set of conditional score functions for different levels of Gaussian noise.

Specifically, given a graph G with its adjacency matrix \mathbf{A} , \mathbf{A} is perturbed with the Gaussian noise of the distribution $q_\sigma(\hat{\mathbf{A}}|\mathbf{A})$:

$$q_\sigma(\hat{\mathbf{A}}|\mathbf{A}) = \prod_{i < j} \frac{1}{\sqrt{2\pi}\sigma} \exp - \frac{(\hat{A}_{i,j} - A_{i,j})^2}{2\sigma^2}, \quad (4)$$

where $\hat{\mathbf{A}}$ represents the perturbed adjacency matrix, and σ is the standard deviation of Gaussian noise. EDP-GNN varies the σ values and obtains a set of noise graphs at different noise intensity levels $\{\sigma_l, \forall l \in [1, L]\}$, where L is the total number of the noise level.

Given the original \mathbf{A} and perturbed adjacency matrices $\hat{\mathbf{A}} = \{\hat{\mathbf{A}}_l, \forall l \in [1, L]\}$ corresponding to the noise set $\{\sigma_l, \forall l \in [1, L]\}$, the objective function of EDP-GNN is to minimize the training loss of the conditional score model $s_\theta(\hat{\mathbf{A}}, \theta)$:

$$\min_{\theta} \frac{1}{2L} \sum_{l=1}^L \sigma_l^2 \mathbb{E} \left[\left\| s_\theta(\hat{\mathbf{A}}_l, \sigma_l) - \frac{\hat{\mathbf{A}}_l - \mathbf{A}}{\sigma_l^2} \right\|_2^2 \right], \quad (5)$$

where \mathbb{E} is the expectation. This objective function can be optimized by an existing optimizer such as SGD [63] and Adam [40].

In this method, C_i trains a set of generative models $\mathcal{M}_i = \{M_{i,k}\}$ for all graph groups. The number of generative models in \mathcal{M}_i is equal to the number of distinct labels in \mathcal{G}_i . Assuming there are N clients participating in FL training, the dataset comprises K classes,

and each diffusion model requires s storage space, the communication bandwidth in terms of the diffusion model for *Basic method* is $N \times K \times s$. Consequently, the communication bandwidth can become substantial with a large number of clients, or numerous classes. Therefore, to reduce the communication bandwidth, we propose an advanced method in which each client C_i only needs to train one generative model. This modification reduces the communication bandwidth to $N \times s'$, with $s \approx s'$. The details of the advanced method are as follows.

4.2.2 Advanced method. The key innovation of the *Advanced method* is incorporating a class label channel during the training of the generative model. This involves adding an embedding layer that takes the data class label as input and outputs a vector of different noise levels for each class label. The noise vector is subsequently employed in both the diffusion forward and reverse processes. By employing this approach, different classes of graphs can be trained with varying noise levels. Specifically, the class label-based embedding layer can be represented as follows:

$$\sigma_k = (\sigma_{1,k}, \sigma_{2,k}, \dots, \sigma_{L,k}) = emb(k), \quad (6)$$

where k represents one of the class labels in the dataset, emb denotes the embedding layer, and L is the pre-defined noise level. Then, the training loss of the diffusion model in Eq. 2 can be modified as:

$$\mathcal{L}(\theta'; \{\sigma_{l,k}\}_{l=1, k=1}^{L, K}) = \min_{\theta'} \frac{1}{2 * L * K} \sum_{k=1}^K \sum_{l=1}^L \sigma_{l,k}^2 \cdot \mathbb{E} \left[\mathbb{1}_{y(x)=k} \left\| s_{\theta'}(\hat{\mathbf{A}}_{l,k}, \sigma_{l,k}) - \nabla_{\hat{\mathbf{A}}_{l,k}} \log q_{\sigma_{l,k}}(\hat{\mathbf{A}}_{l,k} | x) \right\|_2^2 \right], \quad (7)$$

where θ' denotes the parameters of the generative model, K represents the number of class in the dataset, and $y(x)$ indicates the class label of data record x . Accordingly, Formula 5 can be rewritten as:

$$\min_{\theta'} \frac{1}{2 * L * K} \sum_{k=1}^K \sum_{l=1}^L \sigma_{l,k}^2 \cdot \mathbb{E} \left[\mathbb{1}_{y(\mathbf{A})=k} \left\| s_{\theta'}(\hat{\mathbf{A}}_{l,k}, \sigma_{l,k}) - \frac{\hat{\mathbf{A}}_{l,k} - \mathbf{A}}{\sigma_{l,k}^2} \right\|_2^2 \right], \quad (8)$$

where $y(\mathbf{A})$ is the class label of the graph with adjacency matrix \mathbf{A} .

4.3 Phase 2: Generative Model Transferring

After each client C_i obtains his/her locally trained generative models \mathcal{M}_i , he/she uploads \mathcal{M}_i to the server S . To prevent privacy leakage from each client, we require all clients to encrypt their diffusion models using the same encryption mechanism. Subsequently, all the encrypted diffusion models are uploaded to the server, ensuring that the server cannot infer the data information from the clients (the details of our privacy-enhancing method are provided later in Section 6). The server then combines the generative models from all clients, excluding the model from the client itself. After that, the server applies a random shuffle, and distributes the packaged generative models back to the clients, along with the initialization of the GNN. This approach prevents clients from associating the generative models with their respective IDs.

It is worth noting that first, clients are not required to possess samples from all classes. Second, sending generative models instead of generated graphs to server reduces communication bandwidth as well as storage requirements for both server and clients.

Settings	Round 1	Round 2	Round 3	> Round 3	I/O complexity
Traditional FGNNs	$D(GNN) * N / \text{round}$				$D(GNN) * N * S$
CeFGC*	$D(DM) * N$	$D(DM) * (N - 1) * N$	$D(GNN) * N$	-	$D(DM) * N^2 + D(GNN) * N$
CeFGC					

Table 1: Theoretical analysis of communication volume.

4.4 Phase 3: Local GNN Model Training

For each client C_i , let \mathcal{M}_i^S be the generative models C_i receives and decrypts from the server. First, C_i generates a set of synthetic graphs $\hat{\mathcal{G}}_i$, each corresponding to a generative model $M \in \mathcal{M}_i^S$. For each M , C_i can generate multiple graphs that follow the same distribution modeled by M . Next, C_i trains a local GNN model on the training data consisting of all the generated synthetic graphs as well as C_i 's local graphs (i.e., $\hat{\mathcal{G}}_i \cup \mathcal{G}_i$). Finally, C_i uploads the parameters \mathbf{W}_i of the local GNN model to the server.

For generating the synthetic graphs, we adopt the annealed Langevin dynamics sampling algorithm [70]. First, the client randomly samples an integer n , where n is the number of nodes to be generated. Then, it initializes an adjacency matrix $\tilde{\mathbf{A}}^0 \in \mathbb{R}^{n \times n}$ by using the folded norm distribution:

$$\tilde{\mathbf{A}}_{i,j}^0 = |\varepsilon_{i,j}|, \varepsilon_{i,j} \sim \mathcal{N}(0, 1). \quad (9)$$

Then $\tilde{\mathbf{A}}$ is updated by iterative sampling from a series of trained conditional score models $\{s_\theta(\tilde{\mathbf{A}}, \sigma_l)\}_0^L$, which are the generative models C_i receive and decrypt from the server.

So far, the score-based generative model can provide the synthetic sample in the continuous space, whereas the entries in the graph's adjacency matrix are discrete and binary (0/1). To obtain a proper adjacency matrix, we transform the continuous adjacency matrix $\tilde{\mathbf{A}}$ to a binary one: $\tilde{\mathbf{A}}_{i,j}^{final} = \mathbf{1}_{\tilde{\mathbf{A}}_{i,j} > 0.5}$.

As the local GNNs are trained over both synthetic and local graphs that may have different distributions, these models potentially may not be able to converge. However, our empirical studies show that all local GNNs can converge well under different settings.

4.5 Phase 4: Global GNN Model Generation

After collecting all local GNN models from the clients, the server employs an aggregation mechanism to combine them. In this paper, we follow FedAvg [52] and aggregate model weights to construct the global model. Specifically, the weights of the global GNN at l -th layer are computed as follows:

$$\mathbf{W}_{global}^l = \frac{1}{N} \sum_{i=1}^N \mathbf{W}_i^l, \quad (10)$$

where N represents the number of clients, and \mathbf{W}_i^l denotes the weight matrix of local GNN trained by client C_i at l -th layer. Unlike conventional FGNNs, the global GNN in CeFGC is generated through a single aggregation operation rather than multiple iterations of parameter updates. This streamlined approach enhances the efficiency and simplicity of CeFGC. Despite utilizing a single aggregation computation, our empirical results demonstrate its ability to achieve superior performance in graph classification.

Complexity analysis and model artifacts. We refer to our *Basic method* as CeFGC and *Advanced method* as CeFGC* in the following sections. We analyze the efficiency of our models in contrast to the traditional FGNNs such as GCFL+ [79], FedStar [72], in terms of I/O complexity in Table 1. Let $D()$ denote data size, DM the

Algorithm 1: Generative diffusion model based distributed graph classification

Input: Graphs $\mathcal{G}_i, i \in \{1, 2, \dots, N\}$ for each Client i , and the total number of clients is N .
Output: Global model parameters \mathbf{W}_{global}

- 1 **for** $i = 1, 2, \dots, N$ **in parallel for all the clients do**
- 2 Train the generative models M_i for \mathcal{G}_i based on the *basic method* or *advanced method*;
- 3 Encrypt M_i and upload the encrypted M_i to the central server;
- 4 The central server collects all the generative models from the clients, randomly shuffles and aggregates (optional) the generative models, and sends them to the clients.
Meanwhile, the central server sends the initialized global model parameters \mathbf{W}_{global} to each client;
- 5 **for** $i = 1, 2, \dots, N$ **in parallel for all the clients do**
- 6 Decrypt the generative models from the server;
- 7 Generate a set of synthetic graphs $\hat{\mathcal{G}}_i$, each corresponding to a generative model $M \in \mathcal{M}_i^S$;
- 8 Train a local GNN model on the training data consisting of all the generated synthetic graphs as well as C_i 's local graphs (i.e., $\hat{\mathcal{G}}_i \cup \mathcal{G}_i$);
- 9 Upload the local GNN model parameters \mathbf{W}_i to the central server;
- 10 The central server aggregates all the local GNN model parameters \mathbf{W}_i to construct the global GNN model \mathbf{W}_{global} by using FedAvg (Eq. 10);
- 11 **Return** \mathbf{W}_{global}

diffusion model, GNN the used GNN model, N the number of clients, and S the total communication rounds of traditional FGNNs. The I/O costs of CeFGC and CeFGC* per round are $D(DM) * N$, $D(DM) * (N - 1) * N$, $D(GNN) * N$ for the 1st, 2nd, and 3rd round, respectively. Therefore, the overall communication I/O complexity for both CeFGC and CeFGC* is $O(D(DM) * N + D(DM) * (N - 1) * N + D(GNN) * N) = O(D(DM) * N^2 + D(GNN) * N)$. On the contrary, for traditional FGNNs, the model needs a much larger number of rounds $S \gg 3$ case by case, as shown later in Table 3. Each round transmits $D(GNN) * N$ volume. Thus, the I/O complexity is $O(D(GNN) * N * S)$, where a large $S \gg 3$ leads to a lower efficiency in practical applications shown in Table 4. The pseudo-code of our model can be found in Algorithm 1¹.

5 Empirical Evaluation

We conduct a set of empirical studies, aiming to address three key research questions: (1) Q_1 - How effective are CeFGC and CeFGC* on real-world datasets which are non-IID? Q_2 - What are the server-client communication costs of the models? (3) Q_3 - How do the various factors affect the model performance? All the algorithms are implemented in Python with PyTorch and executed on NVIDIA A100-PCIE-40GB.

¹Our code is available at <https://gitfront.io/r/username/5xhoUzcHcPH5/CeFGC/>.

Method	Single-dataset setting					Across-dataset setting					Across-domain setting				
	MUTAG	ENZYMES	PROTEINS	IMDB-B	IMDB-M	Protein		Social		Molecule&Protein&Social		ENZYMES	IMDB-B	IMDB-M	
						ENZYMES	PROTEINS	IMDB-B	IMDB-M	MUTAG	ENZYMES				
FedAvg	0.78	0.55	0.83	0.80	0.75	0.73	0.88	0.72	0.77	0.76	0.71	0.77	0.77	0.69	
FedProx	0.87	0.62	0.83	0.80	0.75	0.70	0.87	0.72	0.75	0.77	0.76	0.69	0.70	0.70	
FedDC	0.78	0.63	0.68	0.74	0.72	0.73	0.86	0.72	0.74	0.79	0.72	0.72	0.72	0.68	
MOON	0.86	0.63	0.71	0.79	0.70	0.72	0.87	0.71	0.76	0.77	0.71	0.73	0.70	0.70	
GCFL+	0.72	0.54	0.75	0.66	0.58	0.71	0.88	0.70	0.77	0.79	0.70	0.71	0.71	0.65	
FedStar	0.72	0.56	0.72	0.57	0.55	0.78	0.69	0.70	0.64	0.90	0.77	0.66	0.80	-	
One-shot	0.72	0.49	0.76	0.54	0.52	-	-	-	-	-	-	-	-	-	
CeFGC	0.91	0.68	0.87	0.81	0.76	0.75	0.89	0.80	0.79	0.88	0.80	0.80	0.80	0.80	
CeFGC*	0.90	0.69	0.87	0.85	0.77	0.79	0.86	0.79	0.78	0.92	0.79	0.78	0.80	0.80	

Table 2: Comparison of global model AUC performance.

5.1 Experimental Setup

Datasets. We use five real-world datasets from three domains: a molecule (MUTAG), two proteins (ENZYMES, PROTEINS), and two social networks (IMDB-BINARY, IMDB-MULTI), each consisting of a set of graphs. These are benchmarks for graph classification [55]. The statistics of these datasets can be found in Appendix A. In the following text, we refer to IMDB-BINARY and IMDB-MULTI as IMDB-B and IMDB-M, respectively. Each dataset uses an 8:2 global train/test split. The global training set is then evenly distributed among three clients, and each client further splits the assigned graphs into train/validate/test sets with a ratio of 0.7/0.1/0.2.

We study three scenarios of distributing data over clients: (1) **Single-dataset** setting: the graphs from a single dataset are randomly distributed across the clients; (2) **Across-dataset** setting: multi datasets from the same domain participate in the global model training, and each client holds the graphs sampled from one dataset (e.g., IMDB-B and IMDB-M datasets); (3) **Across-domain** setting: multi datasets from different domains participate in the global model training, and each client has the graphs sampled from one dataset (e.g., MUTAG and IMDB-B datasets).

We measure the average heterogeneity of features and structures for each setting following [79], with details and analysis provided in Appendix A. Our observations indicate significant heterogeneity across graphs in different settings, confirming their non-IID.

Baselines. We consider two types of baselines, SOTA FL models² and one-shot FL-based method: (1) **SOTA FL models:** FedAvg [52], FedProx [45], GCFL+ [79], FedStar [72], FedDC [17] and MOON [44]. Both FedAvg and FedProx are representative of general FL. FedProx extended FedAvg to address the non-IID issue by adding a proximal term to reduce model differences between local and global models. GCFL+ and FedStar are SOTA FGNNs specifically designed for graph classification with non-IID data. FedDC and MOON are two SOTA FL methods originally developed for non-IID image data, which we have adapted to our graph learning setting. (2) **One-shot FL-based method:** we adapt the one-shot model [21] to our setting, where the server collects all generative models from clients without transferring them back. Instead, the server generates a set of synthetic graphs and trains a global GNN on its own.

Evaluation metrics and parameters. We measure the performance of GNN on graph classification Accuracy and AUC. (1) **Generative models:** We build a 4-layer EDP-GNN³ as the GGDM with the parameter setup in [58]. We use a range of noise scales $\sigma = \{0.1, 0.2, 0.4, 0.6, 0.8, 1.6\}$ for CeFGC and set the number of noise scales to 6 for CeFGC*. (2) **GNN models:** We use the same 3-layer GIN (hidden size 32) for all methods (except FedStar) and follow the configuration in [72] for FedStar.

5.2 Model Performance

In this part of the experiments, we evaluate the graph classification accuracy and AUC of the global model.

Before presenting the results of CeFGC and CeFGC*, we first evaluate the performance of generative diffusion models, both with and without the graph label channel. We evaluate the quality of diffusion models by employing maximum mean discrepancy (MMD) to compare the distributions of graph statistics [7, 32, 36, 49, 58, 89], which are commonly used to assess the model’s performance. The results are available in Appendix B. We observe comparable performance of CeFGC and CeFGC*, suggesting that the diffusion model maintains good quality when the graph label channel is included. Next, we proceed to evaluate the model performance.

Single-dataset setting. Table 2 (“Single-dataset setting” column) presents the graph classification AUC of global model over global testing data for CeFGC, CeFGC*, and baselines. We observe that both CeFGC and CeFGC* consistently achieve high AUC across datasets. For instance, the AUC on MUTAG is 0.91 with CeFGC and 0.90 with CeFGC*. The improvements over the baselines range from 0.01 to 0.31. These results highlight the effectiveness of CeFGC and CeFGC* in the single-dataset setting. Our improvements stem from two aspects: first, the GGDMs can effectively capture the distribution of graphs, allowing the GNN objectives for each local client to align more closely with the global model; and second, the GGDMs enhance the training set with more diverse graphs, increasing the model’s generalization capability. Furthermore, an interesting observation is that the One-shot learning-based model performs poorly in most settings, suggesting that the original graphs play a crucial role in global model training. Therefore, we omit this baseline from the subsequent evaluations.

Across-dataset setting. Table 2 (“Across-dataset setting” column) reports the AUC performance for two across-dataset settings,

²Implementations available at <https://github.com/Oxfordblue7/GCFL> and <https://github.com/yuetan031/FedStar>.

³Implementation available at <https://github.com/ermongroup/GraphScoreMatching>

Method	Communication rounds			Communication volume (Mbit)		
	MUTAG	Social	Mix	MUTAG	Social	Mix
FedAvg	392	392	192	280.00	715.35	700.75
FedProx	416	548	288	297.14	1,000.03	1,051.12
FedDC	375	321	170	267.86	585.786	620.456
MOON	353	301	198	252.14	549.28	722.65
GCFL+	712	200	164	508.57	364.97	598.56
FedStar	360	272	226	560.72	955.10	1,587.15
CeFGC	3			13.90	163.80	537.73
CeFGC*	7.31			69.32	191.29	

Table 3: The number of communication rounds and the communication volume between server and clients under single dataset (MUTAG), across-dataset (Social), and across-domain (Mix) settings.

one with two protein datasets and another with two social networks. We have several observations. First, despite higher heterogeneity in the across-dataset setting, the global model's AUC remains comparable to the single-dataset setting. For instance, when two social networks are distributed, the AUC of IMDB-M dataset is 0.79 with CeFGC and 0.78 with CeFGC*. Second, CeFGC and CeFGC* consistently outperform the six baselines across all settings. For example, CeFGC achieves an increment as high as 14.2% on IMDB-B and 2.6% on IMDB-M compared with GCFL+, while CeFGC* gains 12.9% on IMDB-B and 1.3% on IMDB-M. Third, the performance for some datasets improves in the across-dataset setting compared to the single-dataset setting. For example, when the datasets are from proteins domain, ENZYMES and PROTEINS AUCs rise by 14.5% and 2.3% over single-dataset, which suggests mutual benefits from cross-dataset collaboration.

Across-domain setting. In Table 2 ("Across-domain setting" column), we report global AUCs in a mixed across-domain setting. Notably, both CeFGC and CeFGC* remain consistently effective under across-domain setting, with AUCs comparable to single- and across-dataset settings. Moreover, both CeFGC and CeFGC* consistently outperform all the baselines, showcasing improvements up to 23.1% on IMDB-M. These results demonstrate the efficacy of our models in handling non-IID data. Furthermore, similar to the across-dataset setting, the AUC improves for certain datasets over the single-dataset setting. For example, the AUC MUTAG, ENZYMES, IMDB-M improves by 1.1%, 15.9%, and 3.9%, respectively, compared to the single-dataset setting. Although the performance of IMDB-B drops slightly, the overall average AUC across all four datasets improves by 3.1%. These results indicate that across-domain collaboration is able to enhance each other's performance. This provides an interesting point for further study.

We omit the results of graph classification accuracy under three different settings due to space limits. The observations are similar to those of the AUC performance.

Convergence of local GNN models. As local GNNs are trained over both synthetic and local graphs which may have diverse distributions, we assess their convergence by plotting learning curves. We show the learning curves of local GNNs for the three settings in Appendix C. The convergence condition is defined as no loss decrease within 30 continuous epochs. Overall, local GNNs are well-converged within 500 epochs across all settings. Furthermore, we evaluate local loss values on each client's testing data with local GNN, as well as global model loss on global testing data. We observe that our models consistently outperform the baselines across all

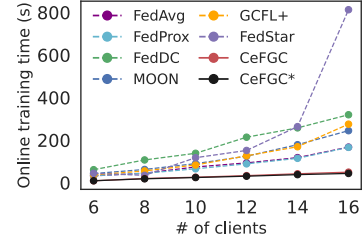


Figure 2: Comparison of total online running time under clients' expansion (seconds) (MUTAG dataset, LAN-45 Mb/s).

settings, in both average local and global loss. Due to space limits, we omit these results. This advocates that the local models in our framework are well-converged and benefit from the generated data.

5.3 Efficiency Evaluation

In this section, we evaluate the efficiency of all competitors in terms of *communication rounds*, *communication volume*, and *online training time*.

Communication rounds. We report the total number of server-client communications rounds for our models and the six baselines under three settings Table 3 ("Communication rounds" column). For the baselines, we count the number of communication rounds until the global model converges, defined as the point when the global loss no longer decreases over 30 consecutive training epochs. We observe that our models significantly reduce the communication rounds from 10^2 to just 3, which demonstrates the superior communication efficiency of our models.

Communication volume. Regarding the communication volume, recall that we provide a theoretical analysis of the data transferred per round as well as the total communication volume for both our models and the baselines in Table 1. We then empirically measure the communication costs across all three experimental settings. The results are presented in Table 3 ("Communication volume" column). We observe that our models significantly reduce the volume of data by 3 to $10^2 \times$ compared to the baselines. This reduction primarily stems from the fact that our models require only three communication rounds.

Online training time. First, we measure the overall online training time of our model, including synthetic graphs generation, local GNN training, server-side aggregation, and client-server data transfer. We exclude the local GGDM training, as it is a one-time, offline process and the trained models are reusable across multiple FL tasks.⁴ Particularly, in dynamic FL settings, existing clients can reuse their GGDMs when new clients join the collaborative learning process. The online time costs of baselines include three main parts: local GNN training, server-side aggregation, and server-client communication cost. We evaluate the server-client data transfer and total time costs under two network conditions: (1) local area network (LAN) with 45 Mb/s bandwidth, (2) wide area network (WAN) with 1 Mb/s. The results in Table 4 show that our model achieves up to 98.0% reduction in running time compared to baselines.

⁴The training times of EDP-GNN-based diffusion models on MUTAG, ENZYMES, IMDB-B, IMDB-M, and PROTEINS are 542, 1,899, 3,537, 4,049, and 3,819 seconds, respectively. It is important to note that our framework is compatible with any GGDMs capable of capturing the original data distribution; newer models such as GDSS or Digrass could further accelerate local diffusion training.

Settings	Single dataset (MUTAG)				Across-dataset (Social)				Across-domain			
	LAN (45 Mb/s)		WAN (1 Mb/s)		LAN (45 Mb/s)		WAN (1 Mb/s)		LAN (45 Mb/s)		WAN (1 Mb/s)	
	T(Trans.)	T(Total)	T(Trans.)	T(Total)	T(Trans.)	T(Total)	T(Trans.)	T(Total)	T(Trans.)	T(Total)	T(Trans.)	T(Total)
FedAvg	24.89	37.24	1,120.00	1,132.35	63.59	140.66	2,861.39	2,939.90	62.29	114.10	2,802.99	2,859.66
FedProx	26.41	42.07	1,188.58	1,204.23	88.89	184.82	4,000.10	4,096.03	93.43	169.22	4,204.49	4,283.77
FedDC	23.08	45.71	1,071.43	1,094.78	52.07	173.97	2,343.13	2,465.59	55.15	193.14	2,481.82	2,619.80
MOON	22.41	40.98	1,008.57	1,028.45	48.83	148.19	2,197.14	2,297.98	64.24	177.92	2,890.58	3,004.27
GCFL+	45.21	78.11	2,034.29	2,067.19	32.44	87.48	1,459.89	1,517.65	53.20	130.98	2,394.22	2,477.14
FedStar	49.84	69.94	2,242.87	2,262.97	84.90	228.66	3,820.39	3,965.47	141.08	313.29	6,348.60	6,521.81
CeFGC	1.24	20.82	55.61	75.20	14.56	58.04	655.19	699.87	47.80	88.41	2,050.92	2,091.09
CeFGC*	0.65	16.02	29.23	44.61	6.16	56.79	277.28	330.91	17.00	79.25	765.15	830.39

Table 4: Comparison of the server-client data transition and total online training time (seconds).

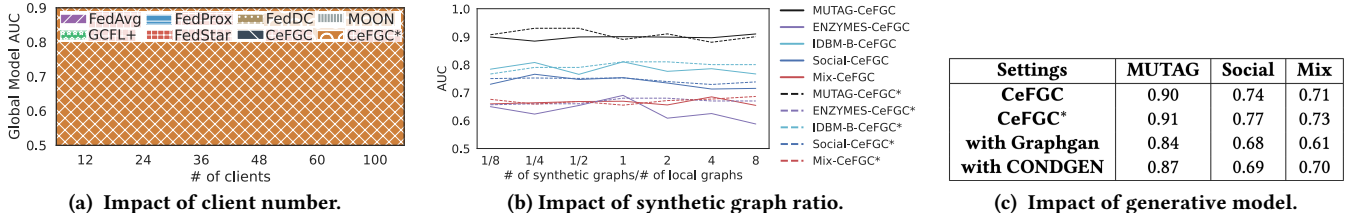


Figure 3: Impact of client numbers, synthetic graph ratios, and incorporation of GANs on global model AUC. "Social" denotes the across-dataset setting involving the IMDB-B and IMDB-M datasets, while 'Mix' refers to the across-domain setting. Figure (a) corresponds to the across-domain setting.

Second, we evaluate the online running time under a dynamic FL setting by progressively increasing the number of clients. For a given dataset, we first evenly and randomly split graphs into 16 clients. We then randomly select an initial subset of 6 clients and expand the client pool to 8, 10, 12, 14, and 16 by incrementally adding clients from the remaining pool. Figure 2 illustrates the online running time as the number of clients increases. Our model consistently runs faster than baselines in all expanded settings.

5.4 Factor Analysis

In this section, we investigate the impact of the number of clients, the number of synthetic graphs, the inclusion of node feature generation, and the use of Generative Adversarial Network (GAN) for graph generation on the performance of our models.

Varying the number of clients. We vary the number of clients to evaluate scalability. We consider client counts of 12, 24, 36, 48, 60, and 100 in the across-domain setting. The first five configurations correspond to mixing datasets from MUTAG, IMDB-B, IMDB-M, and PROTEINS, with each uniformly split into 3, 6, 9, 12, and 15 clients, respectively. The 100-client setting consists of 15 clients from MUTAG, 10 from ENZYMES, and 25 each from PROTEINS, IMDB-B, and IMDB-M. Figure 3a reports the global model AUC on global testing data. We have the following observations. First, both our models and the baselines maintain stable performance as the client count increases, with AUC varying no more than 0.03 and 0.04 for CeFGC and CeFGC*, respectively. Second, our models consistently outperform the baselines across all client counts. We omit the results of the single- and across-dataset due to space limits. The observations mirror those in the across-domain setting.

Varying the number of synthetic graphs. We vary the ratio r between the number of synthetic graphs and the number of the local graphs ($r = 1/8, 1/4, 1/2, 1, 2, 4, 8$), and evaluate the global model AUC on global testing data. From Figure 3b we observe that our model maintains stable performance across all settings, and

there is no consistent pattern between the AUC performance and the ratio between the number of synthetic graphs and the number of local graphs. This is expected as the performance depends on the quality and diversity of the synthetic graphs.

Incorporation of GANs. As GANs have been widely used in the literature for data generation, we replace the generative model in CeFGC with two state-of-the-art graph GANs, Graphgan [74] and CONDGEN [83], and compare graph classification results with diffusion-based models. From Table 3c, we observe that models outperform the GAN-based models. We believe it is contributed to the following reasons: (1) GANs are known to suffer from issues such as mode collapse and training instability, making them difficult to optimize [64]. In contrast, diffusion models offer more stable training by gradually refining the graph structure [69]. (2) Recent studies show that diffusion models outperform GANs in generation quality, mode coverage, and training stability [9, 31, 39].

Effects of node feature generation. We have assessed the performance of our models using the GGDM of EDP-GNN that exclusively generates the graph structure. Now, we extend the evaluation of our models with GGDMs that encompass both node features and graph structure. Specifically, we utilize GDSS model [36], which jointly generates node features and adjacency matrix. Due to space limitations, we omit the global graph classification AUC results here. Our findings indicate no significant difference in the global model performance of CeFGC and CeFGC* between GGDMs that produce only graph structures and those that generate both node features and graph structures, with AUC differences below 0.02. This suggests that incorporating node feature generation has a minimal impact on the performance of CeFGC and CeFGC*.

5.5 Extension to Other Graph Learning Tasks

In the literature, most graph learning applications can be categorized into three major tasks: node classification, link prediction,

Dataset	CeFGC	CeFGC+	CeFGC*	CeFGC*+
PROTEINS (3 clients)	0.87	0.86	0.87	0.86
IMDB-B (3 clients)	0.82	0.83	0.85	0.83
IMDB-M (3 clients)	0.76	0.76	0.77	0.76
Social (6 clients)	0.77	0.74	0.77	0.75
Mix (12 clients)	0.73	0.71	0.74	0.73

Dataset	CeFGC	CeFGC+	CeFGC*	CeFGC*+
PROTEINS (15 clients)	0.81	0.81	0.85	0.83
IMDB-B (15 clients)	0.82	0.83	0.85	0.84
IMDB-M (15 clients)	0.77	0.77	0.76	0.77
Social graphs (30 clients)	0.77	0.77	0.76	0.76
Mix (60 clients)	0.70	0.72	0.69	0.71

Table 5: AUC of the enhanced models. CeFGC+ and CeFGC*+ denote CeFGC and CeFGC* integrated with a privacy-enhancing aggregation mechanism, respectively. "Social graphs" refers to the across-dataset setting with IMDB-B and IMDB-M. "Mix" represents the across-domain setting with Proteins, IMDB-B, and IMDB-M.

and graph classification. Therefore, we extend our model to node classification and link prediction. Specifically, we replace the GIN in our models and baselines with VGAE [41] as the local GNN. We split Cora [66] dataset into three subgraphs via Girvan–Newman algorithm [19], assigning one to each client. Our framework remains effective for link prediction, achieving an AUC of 0.81. Regarding the node classification, since current diffusion-based generators cannot produce node labels, our model does not yet support this task. This limitation highlights labeled graph generation as a promising and important future work.

6 Enhancing the Privacy of Our Model

In both CeFGC and CeFGC*, we enhance the privacy of our model in the following three ways: First, we reduce the number of server-client communication rounds to three, which mitigates the effectiveness of inference attacks [29, 53, 68, 75, 92, 96] and poisoning attacks [4, 50, 56, 85] against FL models, as these attacks typically depend on analyzing gradient or embedding differences across multiple communication rounds. Second, we incorporate encryption techniques in our model that each client shares an encrypted diffusion model with the server, ensuring the privacy of local data. Third, the server randomly shuffles the diffusion models before distributing them to the clients, ensuring that the diffusion models cannot be linked to their respective IDs. However, some curious clients may still attempt to infer data information from the generative models distributed by the server, even though they cannot associate the diffusion models with specific client IDs. Therefore, to enhance the privacy of our model, we employ a key strategy: the server aggregates the generative models within the encryption domain before distributing them to the clients.

First, we need to ensure that computations performed on encrypted data on the server yield the same results as those applied to the original (decrypted) data while providing strong privacy guarantees. To achieve this, we follow previous works [47, 48, 61, 71], allowing the clients in our model to apply Homomorphic Encryption (HE) [2, 18] to encrypt their generative models. HE is popularly adopted in both FL research [13, 51, 59, 80, 87] and related applications such as banking [47], Internet of Things (IoT) systems [28, 88], and medical data analysis [20, 25, 94]. We note that client-server collusion is not considered in this study, as it falls beyond the scope of our work. Since HE ensures equivalent results for computations on both encrypted and decrypted data, we describe the aggregation mechanism as it occurs in the decrypted domain for clarity. The aggregation mechanism proceeds as follows:

First, for each pair of generative model M_i and M_j , where $i \neq j$, the server measures the similarity $sim(M_i, M_j)$ between M_i and M_j with cosine similarity, which can be formulated as:

$$sim(M_i, M_j) = \cos(s_{\theta_i}, s_{\theta_j}), \quad (11)$$

where s represents the conditional score model, θ_i and θ_j are the parameters of the conditional score models for M_i and M_j , respectively. Intuitively, a higher $sim()$ value indicates that the M_i and M_j are more similar to each other.

Second, for each generative model M_i , the server identifies a M_j which is most similar to M_i (i.e., with the largest $sim(M_i, M_j)$). It then averages M_i and M_j to update the parameters of M_i , resulting in an aggregated model \hat{M}_i calculated as:

$$\hat{M}_i = \frac{1}{2} (s_{\theta_i} + s_{\theta_j}). \quad (12)$$

After obtaining \hat{M}_i , for each client, the server packs the aggregated generative models from all clients, excluding the client's own aggregated model. The packed models are randomly shuffled and distributed back to the clients, following the same process described in Phase 2 of Section 4.

Finally, we evaluate the global model AUC performance of CeFGC and CeFGC* with the privacy-enhanced method, denoted as CeFGC+ and CeFGC*+. The evaluation is conducted under single-dataset, across-dataset, and across-domain settings. The results in Table 5 show that the performance of CeFGC+ and CeFGC*+ is comparable to that of CeFGC and CeFGC*, respectively, demonstrating the effectiveness of the enhanced mechanism.

7 Conclusion

Federated GNNs (FGNNs) tackle decentralized graph learning but face two important challenges: i) high communication overhead due to frequent parameter exchanges; ii) non-IID local data among clients. To address these issues, we propose CeFGC and CeFGC*, a novel type of FGNN paradigm that enables training over non-IID data with just three rounds of communication by utilizing generative models. CeFGC and CeFGC* use generative models to minimize direct client-server communication. Each client trains a generative model with or without a graph label channel, encrypts it, and shares it with the server. The server then randomly shuffles and aggregates the uploaded generative models and distributes them back to the clients. Clients generate synthetic graphs based on the generative models from the server, train local GNNs, and upload weights to the server for global aggregation. Extensive experiments and analysis demonstrate the effectiveness and efficiency of our models across diverse settings.

8 Acknowledgments

We thank the anonymous reviewers for their feedback. This work was supported by the Hong Kong RGC Grants C2003-23Y and 12201925.

References

- [1] Sawsan AbdulRahman, Hanine Tout, Azzam Mourad, and Chamseddine Talhi. Fedmcscs: Multicriteria client selection model for optimal iot federated learning. *IEEE Internet of Things Journal*, 8(6):4723–4735, 2020.
- [2] Abbas Acar, Hidayet Aksu, A Selcuk Uluagac, and Mauro Conti. A survey on homomorphic encryption schemes: Theory and implementation. *ACM Computing Surveys (Csur)*, 51(4):1–35, 2018.
- [3] Jacob Austin, Daniel D Johnson, Jonathan Ho, Daniel Tarlow, and Rianne Van Den Berg. Structured denoising diffusion models in discrete state-spaces. *Advances in Neural Information Processing Systems*, 34:17981–17993, 2021.
- [4] Nader Bouacida and Prasant Mohapatra. Vulnerabilities in federated learning. *IEEE Access*, 9:63229–63249, 2021.
- [5] Hanqun Cao, Cheng Tan, Zhangyang Gao, Guangyong Chen, Pheng-Ann Heng, and Stan Z Li. A survey on generative diffusion model. *arXiv preprint arXiv:2209.02646*, 2022.
- [6] Mingzhe Chen, Nir Shlezinger, H Vincent Poor, Yonina C Eldar, and Shuguang Cui. Communication-efficient federated learning. *Proceedings of the National Academy of Sciences*, 118(17):e2024789118, 2021.
- [7] Xiaohui Chen, Yukun Li, Aonan Zhang, and Li-ping Liu. Nvdif: Graph generation through the diffusion of node vectors. *arXiv preprint arXiv:2211.10794*, 2022.
- [8] Yae Jee Cho, Jianyu Wang, and Gauri Joshi. Client selection in federated learning: Convergence analysis and power-of-choice selection strategies. *arXiv preprint arXiv:2010.01243*, 2020.
- [9] Prafulla Dharwal and Alexander Nichol. Diffusion models beat gans on image synthesis. *Advances in neural information processing systems*, 34:8780–8794, 2021.
- [10] Vijay Prakash Dwivedi, Anh Tuan Luu, Thomas Laurent, Yoshua Bengio, and Xavier Bresson. Graph neural networks with learnable structural and positional representations. *arXiv preprint arXiv:2110.07875*, 2021.
- [11] Wenqi Fan, Chengyi Liu, Yunqing Liu, Jiatong Li, Hang Li, Hui Liu, Jiliang Tang, and Qing Li. Generative diffusion models on graphs: Methods and applications. *arXiv preprint arXiv:2302.02591*, 2023.
- [12] Wenqi Fan, Yao Ma, Qing Li, Yuan He, Eric Zhao, Jiliang Tang, and Dawei Yin. Graph neural networks for social recommendation. In *The world wide web conference*, pages 417–426, 2019.
- [13] Haokun Fang and Quan Qian. Privacy preserving machine learning with homomorphic encryption and federated learning. *Future Internet*, 13(4):94, 2021.
- [14] Xingbo Fu, Binchi Zhang, Yushun Dong, Chen Chen, and Jundong Li. Federated graph machine learning: A survey of concepts, techniques, and applications. *ACM SIGKDD Explorations Newsletter*, 24(2):32–47, 2022.
- [15] Chen Gao, Xiang Wang, Xiangnan He, and Yong Li. Graph neural networks for recommender system. In *Proceedings of the Fifteenth ACM International Conference on Web Search and Data Mining*, pages 1623–1625, 2022.
- [16] Chen Gao, Yu Zheng, Nian Li, Yinfei Li, Yingrong Qin, Jinghua Piao, Yuhua Quan, Jianxin Chang, Depeng Jin, Xiangnan He, et al. A survey of graph neural networks for recommender systems: Challenges, methods, and directions. *ACM Transactions on Recommender Systems*, 1(1):1–51, 2023.
- [17] Liang Gao, Huazhu Fu, Li Li, Yingwen Chen, Ming Xu, and Cheng-Zhong Xu. Feddc: Federated learning with non-iid data via local drift decoupling and correction. In *Proceedings of the IEEE/CVF conference on computer vision and pattern recognition*, pages 10112–10121, 2022.
- [18] Craig Gentry. Fully homomorphic encryption using ideal lattices. In *Proceedings of the ACM symposium on Theory of computing*, pages 169–178, 2009.
- [19] Michelle Girvan and Mark EJ Newman. Community structure in social and biological networks. *Proceedings of the national academy of sciences*, 99(12):7821–7826, 2002.
- [20] Alexandros Gkillas, Dimitris Ampeliotis, and Kostas Berberidis. Privacy-preserving federated deep-equilibrium learning for medical image classification. In *IEEE International Symposium on Biomedical Imaging*, pages 1–4, 2024.
- [21] Neel Guha, Ameet Talwalkar, and Virginia Smith. One-shot federated learning. *arXiv preprint arXiv:1902.11175*, 2019.
- [22] Kun Guo, Yutong Fang, Qingqing Huang, Yuting Liang, Ziyao Zhang, Wenyu He, Liu Yang, Kai Chen, Ximeng Liu, and Wenzhong Guo. Globally consistent federated graph autoencoder for non-iid graphs. In *Proceedings of the International Joint Conference on Artificial Intelligence*, pages 3768–3776, 2023.
- [23] Kilian Konstantin Haeferli, Karolis Martinkus, Nathanael Perraudin, and Roger Wattenhofer. Diffusion models for graphs benefit from discrete state spaces. *arXiv preprint arXiv:2210.01549*, 2022.
- [24] William L Hamilton. *Graph representation learning*. Morgan & Claypool Publishers, 2020.
- [25] Stephen Hardy, Wilko Henecka, Hamish Ivey-Law, Richard Nock, Giorgio Patrini, Guillaume Smith, and Brian Thorne. Private federated learning on vertically partitioned data via entity resolution and additively homomorphic encryption. *arXiv preprint arXiv:1711.10677*, 2017.
- [26] Chaoyang He, Keshav Balasubramanian, Emir Ceyani, Carl Yang, Han Xie, Lichao Sun, Lifang He, Liangwei Yang, Philip S Yu, Yu Rong, et al. Fedgraphnn: A federated learning system and benchmark for graph neural networks. *arXiv preprint arXiv:2104.07145*, 2021.
- [27] Chaoyang He, Songze Li, Jinyun So, Xiao Zeng, Mi Zhang, Hongyi Wang, Xiaoyang Wang, Praneeth Vepakomma, Abhishek Singh, Hang Qiu, et al. Fedml: A research library and benchmark for federated machine learning. *arXiv preprint arXiv:2007.13518*, 2020.
- [28] Neveen Mohammad Hijazi, Moayad Aloqaily, Mohsen Guizani, Bassem Ouni, and Fakhri Karray. Secure federated learning with fully homomorphic encryption for iot communications. *IEEE Internet of Things Journal*, 11(3):4289–4300, 2023.
- [29] Briland Hitaj, Giuseppe Ateniese, and Fernando Perez-Cruz. Deep models under the gan: information leakage from collaborative deep learning. In *Proceedings of the ACM SIGSAC conference on computer and communications security*, pages 603–618, 2017.
- [30] Jonathan Ho, Ajay Jain, and Pieter Abbeel. Denoising diffusion probabilistic models. *Advances in neural information processing systems*, 33:6840–6851, 2020.
- [31] Emiel Hoogeboom, Jonathan Heek, and Tim Salimans. simple diffusion: End-to-end diffusion for high resolution images. In *International Conference on Machine Learning*, pages 13213–13232. PMLR, 2023.
- [32] Han Huang, Leilei Sun, Bowen Du, Yanjie Fu, and Weifeng Lv. Graphgdp: Generative diffusion processes for permutation invariant graph generation. In *IEEE International Conference on Data Mining (ICDM)*, pages 201–210, 2022.
- [33] Junxian Huang, Feng Qian, Yihua Guo, Yuanyuan Zhou, Qiang Xu, Z Morley Mao, Subhabrata Sen, and Oliver Spatscheck. An in-depth study of lte: Effect of network protocol and application behavior on performance. *ACM SIGCOMM Computer Communication Review*, 43(4):363–374, 2013.
- [34] Sergey Ivanov and Evgeny Burnaev. Anonymous walk embeddings. In *International conference on machine learning*, pages 2186–2195, 2018.
- [35] Shuting Jin, Xiangxiang Zeng, Feng Xia, Wei Huang, and Xiangrong Liu. Application of deep learning methods in biological networks. *Briefings in bioinformatics*, 22(2):1902–1917, 2021.
- [36] Jaehyeong Jo, Seul Lee, and Sung Ju Hwang. Score-based generative modeling of graphs via the system of stochastic differential equations. In *International Conference on Machine Learning*, pages 10362–10383, 2022.
- [37] Peter Kairouz, H Brendan McMahan, Brendan Avent, Aurélien Bellet, Mehdi Benois, Arjun Nitin Bhagoji, Kalista Bonawitz, Zachary Charles, Graham Cormode, Rachel Cummings, et al. Advances and open problems in federated learning. *Foundations and trends® in machine learning*, 14(1–2):1–210, 2021.
- [38] Michael Kamp, Linara Adilova, Joachim Sicking, Fabian Hüger, Peter Schlicht, Tim Wirtz, and Stefan Wrobel. Efficient decentralized deep learning by dynamic model averaging. In *Joint European Conference on Machine Learning and Knowledge Discovery in Databases*, pages 393–409. Springer, 2019.
- [39] Tero Karras, Miika Aittala, Timo Aila, and Samuli Laine. Elucidating the design space of diffusion-based generative models. *Advances in neural information processing systems*, 35:26565–26577, 2022.
- [40] Diederik P Kingma and Jimmy Ba. Adam: A method for stochastic optimization. *arXiv preprint arXiv:1412.6980*, 2014.
- [41] Thomas N Kipf and Max Welling. Variational graph auto-encoders. *arXiv preprint arXiv:1611.07308*, 2016.
- [42] Jakub Konecný, H Brendan McMahan, Felix X Yu, Peter Richtárik, Ananda Theertha Suresh, and Dave Bacon. Federated learning: Strategies for improving communication efficiency. *arXiv preprint arXiv:1610.05492*, 2016.
- [43] Taku Kudo, Eisaku Maeda, and Yuji Matsumoto. An application of boosting to graph classification. *Advances in neural information processing systems*, 17, 2004.
- [44] Qinbin Li, Bingsheng He, and Dawn Song. Model-contrastive federated learning. In *Proceedings of the IEEE/CVF conference on computer vision and pattern recognition*, pages 10713–10722, 2021.
- [45] Tian Li, Anit Kumar Sahu, Manzil Zaheer, Maziar Sanjabi, Ameet Talwalkar, and Virginia Smith. Federated optimization in heterogeneous networks. *Proceedings of Machine learning and systems*, 2:429–450, 2020.
- [46] Rui Liu, Pengwei Xing, Zichao Deng, Anran Li, Cuntai Guan, and Han Yu. Federated graph neural networks: Overview, techniques and challenges. *arXiv preprint arXiv:2202.07256*, 2022.
- [47] Yang Liu, Tao Fan, Tianjian Chen, Qian Xu, and Qiang Yang. Fate: An industrial grade platform for collaborative learning with data protection. *Journal of Machine Learning Research*, 22(226):1–6, 2021.
- [48] Heiko Ludwig, Nathalie Baracaldo, Gergi Thomas, Yi Zhou, Ali Anwar, Shashank Rajamoni, Yuya Ong, Jayaram Radhakrishnan, Ashish Verma, Mathieu Sinn, et al. Ibm federated learning: an enterprise framework white paper v0. 1. *arXiv preprint arXiv:2007.10987*, 2020.
- [49] Tianze Luo, Zhanfeng Mo, and Sinno Jialin Pan. Fast graph generative model via spectral diffusion. *arXiv preprint arXiv:2211.08892*, 2022.
- [50] Lingjuan Lyu, Han Yu, and Qiang Yang. Threats to federated learning: A survey. *arXiv preprint arXiv:2003.02133*, 2020.
- [51] Jing Ma, Si-Ahmed Naas, Stephan Sigg, and Xiangyang Lyu. Privacy-preserving federated learning based on multi-key homomorphic encryption. *International Journal of Intelligent Systems*, 37(9):5880–5901, 2022.
- [52] Brendan McMahan, Eider Moore, Daniel Ramage, Seth Hampson, and Blaise Aguerre y Arcas. Communication-efficient learning of deep networks from decentralized data. pages 1273–1282, 2017.

[53] Luca Melis, Congzheng Song, Emiliano De Cristofaro, and Vitaly Shmatikov. Exploiting unintended feature leakage in collaborative learning. In *IEEE symposium on security and privacy*, pages 691–706, 2019.

[54] Shengjie Min, Zhan Gao, Jing Peng, Liang Wang, Ke Qin, and Bo Fang. Stgsn—a spatial-temporal graph neural network framework for time-evolving social networks. *Knowledge-Based Systems*, 214:106746, 2021.

[55] Christopher Morris, Nils M Kriege, Franka Bause, Kristian Kersting, Petra Mutzel, and Marion Neumann. Tudataset: A collection of benchmark datasets for learning with graphs. *arXiv preprint arXiv:2007.08663*, 2020.

[56] Virajai Mothukuri, Reza M Parizi, Seyedamin Pouriyeh, Yan Huang, Ali Dehghan-tanha, and Gautam Srivastava. A survey on security and privacy of federated learning. *Future Generation Computer Systems*, 115:619–640, 2021.

[57] Hung T Nguyen, Vikash Sehwag, Seyedali Hosseiniipour, Christopher G Brinton, Mung Chiang, and H Vincent Poor. Fast-convergent federated learning. *IEEE Journal on Selected Areas in Communications*, 39(1):201–218, 2020.

[58] Chenhao Niu, Yang Song, Jiaming Song, Shengjia Zhao, Aditya Grover, and Stefano Ermon. Permutation invariant graph generation via score-based generative modeling. In *International Conference on Artificial Intelligence and Statistics*, pages 4474–4484, 2020.

[59] Jaehyoung Park and Hyuk Lim. Privacy-preserving federated learning using homomorphic encryption. *Applied Sciences*, 12(2):734, 2022.

[60] Amirhossein Reisizadeh, Aryan Mokhtari, Hamed Hassani, Ali Jadbabaie, and Ramin Pedarsani. Fedpaq: A communication-efficient federated learning method with periodic averaging and quantization. In *International Conference on Artificial Intelligence and Statistics*, pages 2021–2031, 2020.

[61] Holger R Roth, Yan Cheng, Yuhong Wen, Isaac Yang, Ziyue Xu, Yuan-Ting Hsieh, Kersten, et al. Nvidia flare: Federated learning from simulation to real-world. *arXiv preprint arXiv:2210.13291*, 2022.

[62] Daniel Rothchild, Ashwinee Panda, Enayat Ullah, Nikita Ivkin, Ion Stoica, Vladimir Braverman, Joseph Gonzalez, and Raman Arora. Fetchsgd: Communication-efficient federated learning with sketching. In *International Conference on Machine Learning*, pages 8253–8265, 2020.

[63] Sebastian Ruder. An overview of gradient descent optimization algorithms. *arXiv preprint arXiv:1609.04747*, 2016.

[64] Tim Salimans, Ian Goodfellow, Wojciech Zaremba, Vicki Cheung, Alec Radford, and Xi Chen. Improved techniques for training gans. *Advances in neural information processing systems*, 29, 2016.

[65] Felix Sattler, Simon Wiedemann, Klaus-Robert Müller, and Wojciech Samek. Robust and communication-efficient federated learning from non-iid data. *IEEE transactions on neural networks and learning systems*, 31(9):3400–3413, 2019.

[66] Prithviraj Sen, Galileo Namata, Mustafa Bilgic, Lise Getoor, Brian Gallagher, and Tina Eliassi-Rad. Collective classification in network data. *AI magazine*, 29(3):93–93, 2008.

[67] Osama Shahid, Seyedamin Pouriyeh, Reza M Parizi, Quan Z Sheng, Gautam Srivastava, and Liang Zhao. Communication efficiency in federated learning: Achievements and challenges. *arXiv preprint arXiv:2107.10996*, 2021.

[68] Reza Shokri, Marco Stronati, Congzheng Song, and Vitaly Shmatikov. Membership inference attacks against machine learning models. In *IEEE symposium on security and privacy*, pages 3–18, 2017.

[69] Jascha Sohl-Dickstein, Eric Weiss, Niru Maheswaranathan, and Surya Ganguli. Deep unsupervised learning using nonequilibrium thermodynamics. In *International conference on machine learning*, pages 2256–2265. pmlr, 2015.

[70] Yang Song and Stefano Ermon. Generative modeling by estimating gradients of the data distribution. *Advances in neural information processing systems*, 32, 2019.

[71] Dimitris Stripelis, Hamza Saleem, Tanmay Ghai, Nikhil Dhinagar, Umang Gupta, Chrysoualantis Anastasiou, Greg Ver Steeg, Srivatsan Ravi, Muhammad Naveed, Paul M Thompson, et al. Secure neuroimaging analysis using federated learning with homomorphic encryption. In *International Symposium on medical information processing and analysis*, volume 12088, pages 351–359. SPIE, 2021.

[72] Yue Tan, Yixin Liu, Guodong Long, Jing Jiang, Qinghua Lu, and Chengqi Zhang. Federated learning on non-iid graphs via structural knowledge sharing. In *Proceedings of the AAAI conference on artificial intelligence*, volume 37, pages 9953–9961, 2023.

[73] Clement Vignac, Igor Krawczuk, Antoine Siraudin, Bohan Wang, Volkan Cevher, and Pascal Frossard. Digrss: Discrete denoising diffusion for graph generation. *arXiv preprint arXiv:2209.14734*, 2022.

[74] H Wang, J Wang, J Wang, et al. Graph representation learning with generative adversarial nets. *AAAI, Graphgan*, 2017.

[75] Zhibo Wang, Mengkai Song, Zhifei Zhang, Yang Song, Qian Wang, and Hairong Qi. Beyond inferring class representatives: User-level privacy leakage from federated learning. In *IEEE INFOCOM conference on computer communications*, pages 2512–2520, 2019.

[76] Chuhuan Wu, Fangzhao Wu, Yang Cao, Yongfeng Huang, and Xing Xie. Fedggn: Federated graph neural network for privacy-preserving recommendation. *arXiv preprint arXiv:2102.04925*, 2021.

[77] Hongda Wu and Ping Wang. Fast-convergent federated learning with adaptive weighting. *IEEE Transactions on Cognitive Communications and Networking*, 7(4):1078–1088, 2021.

[78] Zonghan Wu, Shirui Pan, Fengwen Chen, Guodong Long, Chengqi Zhang, and S Yu Philip. A comprehensive survey on graph neural networks. *IEEE transactions on neural networks and learning systems*, 32(1):4–24, 2020.

[79] Han Xie, Jing Ma, Li Xiong, and Carl Yang. Federated graph classification over non-iid graphs. *Advances in Neural Information Processing Systems*, 34:18839–18852, 2021.

[80] Qipeng Xie, Siyang Jiang, Linshan Jiang, Yongzhi Huang, Zhihe Zhao, Salabat Khan, Wangchen Dai, Zhe Liu, and Kaishun Wu. Efficiency optimization techniques in privacy-preserving federated learning with homomorphic encryption: A brief survey. *IEEE Internet of Things Journal*, 11(14):24569–24580, 2024.

[81] Jie Xu and Heqiang Wang. Client selection and bandwidth allocation in wireless federated learning networks: A long-term perspective. *IEEE Transactions on Wireless Communications*, 20(2):1188–1200, 2020.

[82] Keyulu Xu, Weihua Hu, Jure Leskovec, and Stefanie Jegelka. How powerful are graph neural networks? *arXiv preprint arXiv:1810.00826*, 2018.

[83] Carl Yang, Peiye Zhuang, Wenhan Shi, Alan Luu, and Pan Li. Conditional structure generation through graph variational generative adversarial nets. *Advances in neural information processing systems*, 32, 2019.

[84] Ling Yang, Zhilong Zhang, Yang Song, Shenda Hong, Runsheng Xu, Yue Zhao, Wentao Zhang, Bin Cui, and Ming-Hsuan Yang. Diffusion models: A comprehensive survey of methods and applications. *ACM Computing Surveys*, 56(4):1–39, 2023.

[85] Xuefei Yin, Yanming Zhu, and Jiankun Hu. A comprehensive survey of privacy-preserving federated learning: A taxonomy, review, and future directions. *ACM Computing Surveys*, 54(6):1–36, 2021.

[86] Zhitao Ying, Jiaxuan You, Christopher Morris, Xiang Ren, Will Hamilton, and Jure Leskovec. Hierarchical graph representation learning with differentiable pooling. *Advances in neural information processing systems*, 31, 2018.

[87] Chengliang Zhang, Suyi Li, Junzhe Xia, Wei Wang, Feng Yan, and Yang Liu. {BatchCrypt}: Efficient homomorphic encryption for {Cross-Silo} federated learning. In *USENIX annual technical conference*, pages 493–506, 2020.

[88] Li Zhang, Jianbo Xu, Pandi Vijayakumar, Pradip Kumar Sharma, and Uttam Ghosh. Homomorphic encryption-based privacy-preserving federated learning in iot-enabled healthcare system. *IEEE transactions on network science and engineering*, 10(5):2864–2880, 2022.

[89] Mengchun Zhang, Maryam Qamar, Taegoo Kang, Yuna Jung, Chenshuang Zhang, Sung-Ho Bae, and Chaoning Zhang. A survey on graph diffusion models: Generative ai in science for molecule, protein and material. *arXiv preprint arXiv:2304.01565*, 2023.

[90] Muhan Zhang, Zhicheng Cui, Marion Neumann, and Yixin Chen. An end-to-end deep learning architecture for graph classification. In *Proceedings of the AAAI conference on artificial intelligence*, volume 32, 2018.

[91] Shijie Zhang, Hongzhi Yin, Tong Chen, Zi Huang, Lizhen Cui, and Xiangliang Zhang. Graph embedding for recommendation against attribute inference attacks. In *Proceedings of the Web Conference 2021*, pages 3002–3014, 2021.

[92] Bo Zhao, Konda Reddy Mopuri, and Hakan Bilen. idlg: Improved deep leakage from gradients. *arXiv preprint arXiv:2001.02610*, 2020.

[93] Jie Zhou, Ganqu Cui, Shengding Hu, Zhengyan Zhang, Cheng Yang, Zhiyuan Liu, Lifeng Wang, Changcheng Li, and Maosong Sun. Graph neural networks: A review of methods and applications. *AI open*, 1:57–81, 2020.

[94] Juxiao Zhou, Longxi Zhou, Di Wang, Xiaopeng Xu, Haoyang Li, Yuetan Chu, Wenkai Han, and Xin Gao. Personalized and privacy-preserving federated heterogeneous medical image analysis with pppml-hmi. *Computers in Biology and Medicine*, 169:107861, 2024.

[95] Yanlin Zhou, George Pu, Xiyao Ma, Xiaolin Li, and Dapeng Wu. Distilled one-shot federated learning. *arXiv preprint arXiv:2009.07999*, 2020.

[96] Ligeng Zhu, Zhijian Liu, and Song Han. Deep leakage from gradients. *Advances in neural information processing systems*, 32, 2019.

Appendix

A Details of Datasets

Statistics of datasets. We use five real-world datasets for graph classification in our paper, namely MUTAG, ENZYMES, PROTEINS, IMDB-BINARY, and IMDB-MULTI⁵, which serve as benchmarks for evaluating graph-based models in various domains [55]. Table 6 provides details of these datasets.

Non-IID distribution. We measure the average heterogeneity of features and structures for each setting and include the results in

⁵All the datasets are downloaded from torch_geometric package. For IMDB-BINARY and IMDB-MULTI datasets that do not have node features, we follow [79] and use one-hot degree features as the node features.

Dataset	Domain	# Graphs	Avg. # Nodes	Avg. # Edges	Avg. # Degrees	# Node features	# Classes
MUTAG	Molecules	188	17.93	19.79	2.11	7	2
ENZYMES	Proteins	600	32.60	124.3	7.63	3	6
PROTEINS	Proteins	1,113	39.06	72.82	3.73	3	2
IMDB-BINARY	Social network	1,000	19.77	96.53	9.77	135	2
IMDB-MULTI	Social network	1,500	13.00	65.94	10.14	88	3

Table 6: Statistics of datasets

Settings	Single dataset					Across-dataset		Across-domain	
	MUTAG	PROTEINS	ENZYMES	IMDB-B	IMDB-M	Protein	Social	Molecular&Protein&Social	
						PROTEINS &ENZYMES	IMDB-B &IMDB-M	MUTAG&ENZYMES &IMDB-B&IMDB-M	
Avg. Struc. hetero.	0.16(±0.02)	0.28(±0.06)	0.28(±0.05)	0.27(±0.05)	0.28(±0.05)	0.37(±0.13)	0.28(±0.22)	0.39(±0.20)	
Avg. Feat. hetero.	0.13(±0.09)	0.13(±0.10)	0.16(±0.12)	0.18(±0.12)	0.19(±0.15)	0.15(±0.11)	0.15(±0.13)	0.21(±0.13)	

Table 7: Heterogeneity for different settings between different clients.

Settings	MUTAG dataset								PROTEINS dataset							
	k=1				k=2				k=1				k=2			
	Deg.↓	Clus.↓	Orb.↓	Avg.↓	Deg.↓	Clus.↓	Orb.↓	Avg.↓	Deg.↓	Clus.↓	Orb.↓	Avg.↓	Deg.↓	Clus.↓	Orb.↓	Avg.↓
w/o	0.032	0.122	0.004	0.052	0.004	0.131	0.001	0.045	0.137	0.704	0.443	0.428	0.276	0.387	0.147	0.270
with	0.047	0.103	0.019	0.057	0.032	0.040	0.030	0.034	0.179	0.645	0.427	0.417	0.257	0.324	0.257	0.279

Table 8: Quality of the generative diffusion models with or without the graph label channel. Deg., Clus., and Orb. represent the MMD values in terms of degree distribution, clustering coefficients, and the number of occurrences of orbits with 4 nodes, respectively, and Avg. denotes the average MMD value across Deg., Clus., and Orb.

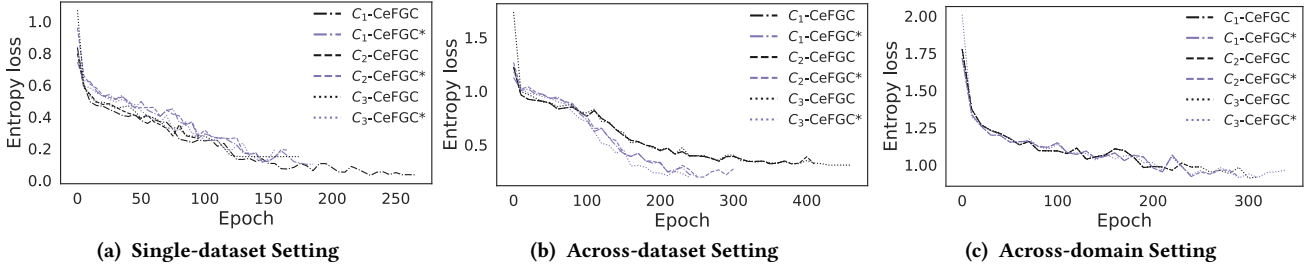


Figure 4: Convergence analysis of local GNN models through the learning curve (IMDB-B dataset).

Table 7. For structure heterogeneity, first, we train the graph embedding for each graph with Anonymous Walk Embeddings (AWEs) [34, 79]. Second, for each pair of clients, we calculate the Jensen-Shannon (JS) distance between the AWEs of each graph pair across the two clients. Third, we calculate the structure heterogeneity as the average JS distance across all graph pairs for all client pairs. For feature heterogeneity, we first calculate the feature similarity of the linked edges within each graph with cosine similarity. Second, for each pair of clients, we compute the JS distance between the feature similarity of each graph pair across the two clients. Finally, we assess feature heterogeneity as the average JS distance across all graph pairs for all client pairs. From Table 7, we observe significant heterogeneity in all three settings (i.e., the data follows the non-IID distribution in the three settings). Furthermore, the structure heterogeneity increases from the single-dataset setting to across-datasets setting, and across-domains setting. For example, the structure heterogeneity values for PROTEINS and ENZYMES are 0.28 in the single-dataset setting, but increase to 0.37 in the across-dataset setting and 0.39 in the across-domain setting.

B Performance of the Generative Diffusion Models with and without the Graph Label Channel

By following [7, 32, 36, 49, 58, 89], we assess the quality of the diffusion model by using maximum mean discrepancy (MMD) to compare the distributions of graph statistics, such as the degree, the clustering coefficient, and the number of occurrences of orbits with 4 nodes between the same number of generated and test graphs. As shown in Table 8, we observe the comparable diffusion model performance with and without the graph label channel, demonstrating that the model retains its quality with the inclusion of the graph label channel.

C Convergence of Local GNN Models under Three Settings

Figure 4 exhibits the learning curves of local GNNs under the single-dataset, across-dataset, and across-domain settings on IMDB-B. We observe that all local GNNs are well-converged within 500 epochs.